Laser-driven generation of collimated ultra-relativistic positron beams

2013 Plasma Phys. Control. Fusion 55 124017

(http://iopscience.iop.org/0741-3335/55/12/124017)

Plasma Phys. Control. Fusion **55** (2013) 124017 (6pp) doi:10.1088/0741-3335/55/12/124017

Laser-driven generation of collimated ultra-relativistic positron beams

G Sarri[1], W Schumaker[2], A Di Piazza[3], K Poder[4], J M Cole[4], M Vargas[2], D Doria[1], S Kushel[5], B Dromey[1], G Grittani[6], L Gizzi[6], M E Dieckmann[7], A Green[1], V Chvykov[2], A Maksimchuk[2], V Yanovsky[2], Z H He[2], B X Hou[2], J A Nees[2], S Kar[1], Z Najmudin[4], A G R Thomas[2], C H Keitel[3], K Krushelnick[2] and M Zepf[1,5]

[1] School of Mathematics and Physics, The Queen's University of Belfast, BT7 1NN, Belfast, UK
[2] Center for Ultrafast Optical Science, University of Michigan, Ann Arbor, MI 48109-2099, USA
[3] Max-Planck-Institut für Kernphysik, Saupfercheckweg 1, 69117 Heidelberg, Germany
[4] Imperial College of Science, Technology and Medicine, London SW7 2BZ, UK
[5] Helmholtz Institute Jena, Fröbelstieg 3, 07743 Jena, Germany
[6] Istituto Nazionale di Ottica, Consiglio Nazionale delle Ricerche, 56124 Pisa, Italy
[7] Department of Science and Technology (ITN), Linköpings University, Campus Norrköping, SE-60174 Norrköping, Sweden

Received 3 July 2013, in final form 11 October 2013
Published 28 November 2013
Online at stacks.iop.org/PPCF/55/124017

Abstract
We report on recent experimental results concerning the generation of collimated (divergence of the order of a few mrad) ultra-relativistic positron beams using a fully optical system. The positron beams are generated exploiting a quantum-electrodynamic cascade initiated by the propagation of a laser-accelerated, ultra-relativistic electron beam through high-Z solid targets. As long as the target thickness is comparable to or smaller than the radiation length of the material, the divergence of the escaping positron beam is of the order of the inverse of its Lorentz factor. For thicker solid targets the divergence is seen to gradually increase, due to the increased number of fundamental steps in the cascade, but it is still kept of the order of few tens of mrad, depending on the spectral components in the beam. This high degree of collimation will be fundamental for further injection into plasma-wakefield afterburners.

(Some figures may appear in colour only in the online journal)

1. Introduction

The generation of ultra-relativistic and high-quality positron beams in the laboratory is a field of research of paramount importance due to its direct relevance to a wide range of physical subjects, which include nuclear and particle physics, laboratory astrophysics, and plasma physics. Due to the obvious difficulties encountered in generating stable antimatter, and in further accelerating it to ultra-relativistic energies, this field of research has thus far been prerogative of large-scale conventional accelerators, such as the recently dismissed Large Electron–Positron Collider (LEP) [1], or the Stanford Linear Accelerator (SLAC) [2]. Positron beams with energy as high as 100 GeV have been obtained at LEP, which contributed towards fundamental advancements in nuclear and particle physics. In its basic configuration, an electron beam was accelerated by a linear accelerator (LINAC) up to 200 MeV. This electron beam impacted onto a tungsten target and generated a high-density population of relatively low-energy positrons. After due storage, these positrons were then accelerated up to approximately 100 GeV in a km scale synchrotron. However, such a large size and subsequent high cost of these machines is motivating the quest for alternative acceleration schemes; in this context, plasma devices are appealing candidates due to the extremely high accelerating fields that they are able to support (of the order of 100 s of GV m^{-1}, compared to the typical MV m^{-1} obtainable in conventional accelerators). Laser–plasma accelerators have already demonstrated the generation of electron beams with energy per particle reaching [3], if not exceeding [4], 1 GeV and energies per particles approaching 100 GeV are theoretically

predicted for the next class of high-power ($\simeq$10 PW) laser systems [5]. Moreover, particle-driven plasma-wakefield afterburners have been recently demonstrated to represent a compact (meter-scale) and powerful device for further beam acceleration [6].

On the other hand, laser-driven high-energy positron beams are much harder to generate. Researchers from the Lawrence Livermore National Laboratory (LLNL) demonstrated the possibility of generating a population of relativistic positrons by focusing a kJ-class laser on a mm-thick gold target [7]. Despite the intrinsic interest of these results, a major drawback is represented by the broad divergence of these beams (cone aperture of $\theta_{\mathrm{LLNL}} \simeq 20^{\circ}$), which prevents from efficient storage and further acceleration. Arguably, the easiest way to generate a significant population of positrons is to exploit the electromagnetic cascade initiated by an ultra-relativistic electron beam propagating though a solid target. This is the physical phenomenon exploited also in the positron generation stage in conventional accelerators, such as LEP [1]. It is intuitive that the resulting positron beam would present a divergence whose lower limit is given by the divergence of the primary electron beam. In the LLNL experiment, the impact of the laser pulse onto the gold target generated, inside it, a broadly divergent electron beam ($\theta_{\mathrm{e}^-} \simeq 20^{\circ}$), as expected for this sort of generation mechanism. Hence, the subsequently generated positrons preserved the same degree of divergence. An alternative solution is obtained if the electron generation and the electromagnetic shower producing the positrons are separated into two different stages. This idea was first brought forward by Gahn and collaborators [8]. In that work, the electrons were first generated during the interaction of a low-intensity laser pulse with a gaseous target; the generated electron beam subsequently triggered an electromagnetic shower during propagation through a high-Z solid target. However, the low intensity of the laser available at the time, together with a non-optimized electron generation in the gas, did not allow for a better degree of collimation; a divergence of the order of 20° was in fact reported.

Since this proof-of-principle experiment, laser-driven electron acceleration has dramatically improved; collimated ($\theta_{\mathrm{LWFA}} \simeq$ 1–2 mrad $\simeq 0.06^{\circ}$) and high-energy ($E_{\mathrm{LWFA}} \simeq$ GeV) electron beams can now be generated when a high-intensity laser pulse propagates through a gaseous target, exploiting a physical mechanism known as laser wakefield acceleration (LWFA) [9]. In this article, we show that, combining the recent improvements in laser-wakefield electron acceleration with the proof-of-principle idea introduced by Gahn and collaborators, collimated ultra-relativistic positron beams (divergence of the order of a few mrad and energy of the order of hundreds of MeV) can be generated in a relatively small-scale laser-driven setup. We envisage that these positron beams would be of interest for a wide range of practical applications. First of all, such a low divergence obtained is indeed encouraging towards the further acceleration of these beams with plasma afterburners (an idea first experimentally tested by Blumenfeld and collaborators [6]). Moreover, the high density obtained makes laboratory-based studies of astrophysically relevant electron–positron-ion plasma phenomena finally accessible. A thorough characterization of this physical scenario is indeed necessary in order to advance our understanding of astrophysical jets, which have been observed to be ejected by some of the most powerful or compact objects in the known Universe, such as black holes, pulsars, and quasars [10]. Finally, these results promote the idea of the near-term construction of GeV laser-driven electron–positron colliders. These machines would finally provide a relatively cheap platform for experimental studies of nuclear and particle physics, making this branch of experimental physics finally widely accessible on a University level.

The article is organized as follows: section 2 will briefly describe the physics underlying the quantum-electrodynamic cascade initiated by an ultra-relativistic electron beam in a high-Z solid. Section 3 will discuss the experimental evidence of ultra-relativistic positron beams with a few mrad divergence if solid targets with a thickness comparable to or smaller than the radiation length of the material is used. Section 4 will instead show that the positron divergence increases if thicker solid targets are used, but that it will still remain of the order of 10–20 mrad ($\simeq 1^{\circ}$). Finally, a conclusive paragraph will be provided by section 5.

2. QED electromagnetic showers: a simple model

The production of cascade showers during the passage of high-energy particles through matter have been investigated for a long time and we refer here to the classic textbook [11]. We limit to quantum-electrodynamic cascades involving only electrons, positrons and photons at energies much larger than the electron rest energy m (units where $\hbar = c = 1$ are employed in this section). In particular, we assume that the cascade is initiated by a pencil-like beam of electrons propagating perpendicularly to the target. At ultra-relativistic energies, the cascade can be assumed to propagate essentially along the initial direction of propagation of the electron beam [11]. Thus, the electron/positron distribution functions $f_{\mp}(E, d)$ and the photon distribution function $f_{\gamma}(E, d)$ depend only on the energy E and on the thickness d of the target. At ultra-relativistic energies, one can in first approximation neglect electron and positron energy losses as resulting from Compton scattering with the electrons of the fixed atoms and from the ionization of the fixed atoms at the passage of the cascade. In this case, the only processes to be included in the kinetic equations describing the evolution of the cascade are the emission of photons by electrons and positrons via bremsstrahlung [12] and the creation of an electron–positron pair by a photon [13], both processes occurring in the field of a heavy atom. It is useful to rescale the target thickness d in terms of the radiation length of the material. For an order of magnitude estimate of L_{rad}, we can assume here to be in the total-screening regime which, for an electron with energy ε emitting a photon with energy ω, occurs if the parameter $S \equiv \alpha Z^{1/3}\varepsilon(\varepsilon - \omega)/(\omega m)$ is much larger than unity (here, $\alpha \approx 1/137$ is the fine structure constant, m is the rest mass of the electron and a Thomas-Fermi model of the atom is assumed [13]). In this regime, and by including Coulomb

corrections, the radiation length is approximately given by [13]: $L_{\rm rad} \approx 1/[4\alpha(Z\alpha)^2 n\lambda_{\rm C}^2 L_0]$, where n is the number of atoms per unit volume, $\lambda_{\rm C} = 1/m = 3.9 \times 10^{-11}$ cm is the Compton wavelength, and $L_0 = \log(183Z^{-1/3}) - f(Z\alpha)$, with $f(x) = \sum_{\ell=1}^{\infty} x^2/\ell(\ell^2 + x^2)$. The radiation lengths of Pb and Ta are thus, respectively: $L_{\rm rad}({\rm Pb}) = 5.6$ mm and $L_{\rm rad}({\rm Ta}) = 4.1$ mm. By setting δ as the target thickness d in units of the radiation length $L_{\rm rad}$, i.e. $\delta = d/L_{\rm rad}$, the kinetic equations can be approximately written as [11]

$$\frac{\partial f_\pm}{\partial \delta} = -\int_0^1 {\rm d}v \psi_{\rm rad}(v)\left[f_\pm(E,\delta) - \frac{1}{1-v} f_\pm\left(\frac{E}{1-v},\delta\right)\right] + \int_0^1 \frac{{\rm d}v}{v}\psi_{\rm pair}(v) f_\gamma\left(\frac{E}{v},\delta\right), \quad (1)$$

$$\frac{\partial f_\gamma}{\partial \delta} = \int_0^1 \frac{{\rm d}v}{v}\psi_{\rm rad}(v)\left[f_-\left(\frac{E}{v},\delta\right) + f_+\left(\frac{E}{v},\delta\right)\right] - \mu_0 f_\gamma(E,\delta), \quad (2)$$

where the functions

$$\psi_{\rm rad}(v) = \frac{1}{v}\left[1 + (1-v)^2 - (1-v)\left(\frac{2}{3} - 2b\right)\right], \quad (3)$$

$$\psi_{\rm pair}(v) = v^2 + (1-v)^2 + v(1-v)\left(\frac{2}{3} - 2b\right), \quad (4)$$

$$\mu_0 = \frac{7}{9} - \frac{b}{3}, \quad (5)$$

with $b = 1/18\log(183/Z^{1/3})$, are related to the cross section of bremsstrahlung and pair photo-production in the field of a heavy atom with charge number Z (see [11] for details). The electron and the positron distribution enter symmetrically in the above equations. As an example, figure 1 depicts the calculated number of ultra-relativistic electrons and positrons ($E > 120$ MeV) generated once an electron beam with a flat spectrum ranging from 120 MeV to 1 GeV (total number of electrons: 2.7×10^9) propagates through a Pb target of different δ. As we can see, a maximum in positron number ($N_{\rm p} \simeq 2.5 \times 10^8$) is obtained for $\delta \approx 2$. Increasing the target thickness above this value, induces a net decrease in positron yield. This can be intuitively understood by noting that, for such thick targets, there is a higher probability that any generated positron within the target might undergo an energy loss during the propagation through the rest of the solid.

Due to the ultra-relativistic nature of the particles involved, the divergence of the electrons and positrons escaping the target is expected to be inversely proportional to their Lorentz factor. If the target thickness is less or equal to the radiation length of the material, the average cone angle is given by $\langle\theta_{\rm e^+}^2\rangle \approx 1/\gamma_{\rm e^+}^2$ [13]. For thicker targets instead, a multiple step cascade is likely to occur, and the average cone angle can be estimated as [14]

$$\sqrt{\langle\theta_{\rm e^+}^2\rangle} \approx \frac{19.2\,{\rm MeV}/c}{p}\sqrt{\delta}, \quad (6)$$

with p being the momentum of the particle. Again, the inverse proportionality with the particle Lorentz factor is preserved even though the divergence increases with the square root of the target thickness.

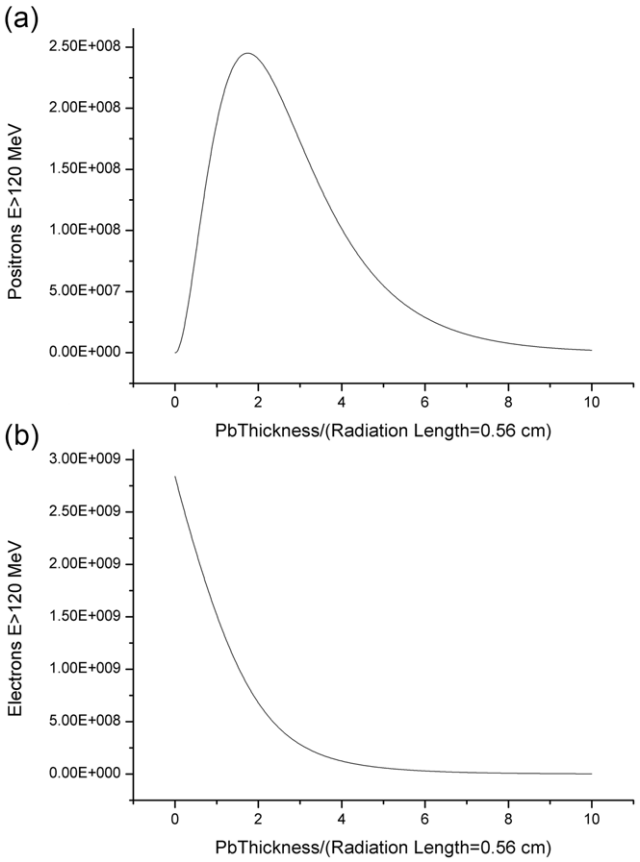

Figure 1. Calculated number of ultra-relativistic ($E > 120$ MeV) positrons (*a*) and electrons (*b*) escaping a Pb target of different thicknesses δ once an electron beam with a flat spectrum ranging from 120 MeV to 1 GeV (total number of electrons: 2.7×10^9) propagates through it.

3. Positron beam divergence if $\delta \leqslant 1$

In this section, we will discuss in detail the divergence of the positron beams obtained in an experimental campaign carried out at the HERCULES laser [15], hosted by the Centre for Ultrafast Optical Science at the University of Michigan, US. A detailed description of the experiment, together with the energy spectrum and density of the positron beams obtained can be found in [16]; however, we will repeat part of it here, for the sake of clarity. A sketch of the experimental setup is depicted in figure 2(*a*). A laser beam with energy $E_{\rm L} = 0.8$ J and duration $\tau_{\rm L} = 30$ fs was focused (peak intensity of $I_{\rm L} \approx 6 \times 10^{18}$ W cm^{-2}) onto the edge of a 3 mm wide supersonic He gas-jet, doped with 2.5% of N_2. Once fully ionized, the electron density inside the gas-jet was 9×10^{18} cm^{-3}. This interaction delivered, via ionization injection [17], a reproducible electron beam with a divergence with a full-width half-maximum of 1.4 mrad and a broad spectrum extending to approximately 200 MeV (see figure 2(*b*)). The laser-accelerated electron beam interacted with mm-size high-Z solid targets of different materials (Cu, Sn, Ta, Pb) and thicknesses (from 1.4 to 6.4 mm). However, we will concentrate here only on the results obtained using 2.8 mm and 4.1 mm of Ta. A magnetic spectrometer was used to separate the electrons and positrons which were then recorded on a LANEX screen and an Image Plate, respectively.

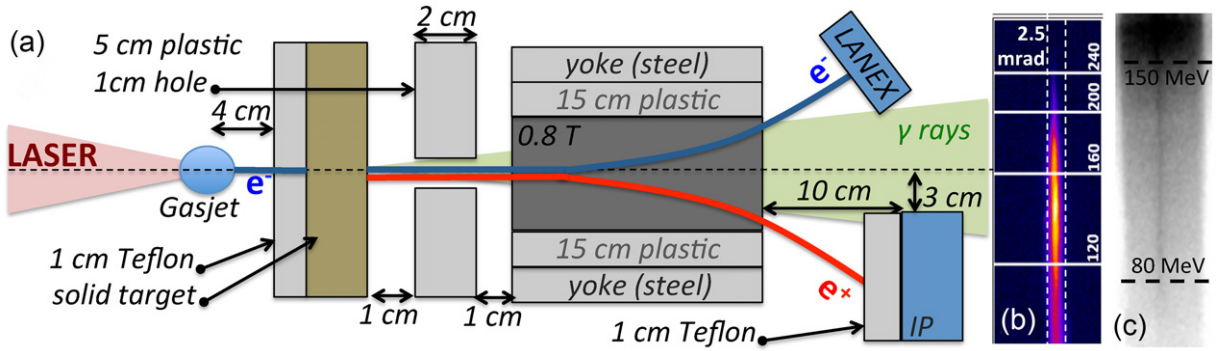

Figure 2. (*a*) Sketch of the experimental setup adopted at the HERCULES laser. (*b*) Typical electron signal on the LANEX screen if no solid target is inserted in the electron beam path. The full-width total maximum of the electron beam divergence is 2.5 mrad, corresponding to a full-width half-maximum of 1.4 mrad. Details of the resulting electron spectrum and charge can be found in [16]. (*c*) Typical positron signal on the Image Plate if 4.1 mm of Ta are inserted in the electron beam path. The corresponding positron spectrum can be found in [16]. The beam presents a divergence of the order of 3–4 mrad, depending on the spectral component of the beam. Figures 1(*b*) and (*c*) are adapted from [16].

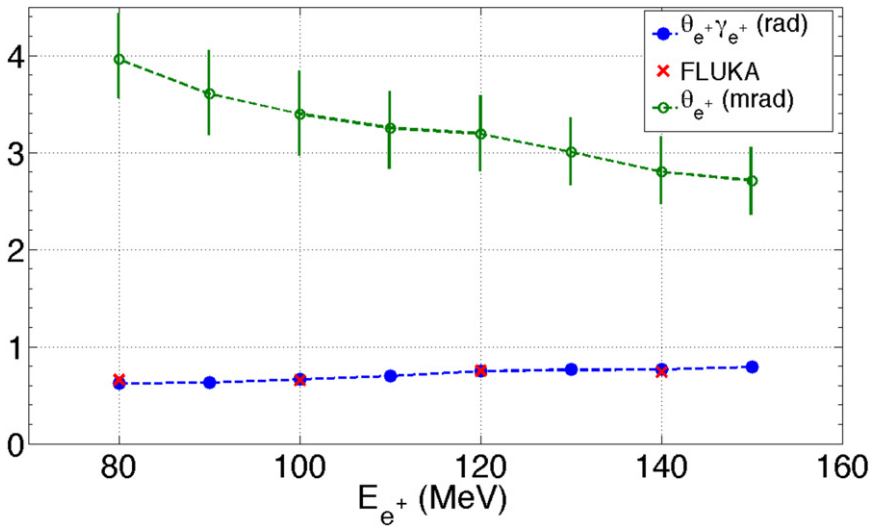

Figure 3. Divergence of the positron beam escaping from 4.1 mm of Ta as a function of the positron energy. Empty green circles depict the measured divergence in mrad (θ_{e^+}), solid blue circles and red crosses indicate the measured and simulated product $\theta_{e^+}\gamma_{e^+}$, respectively. 2.8 mm of Ta provided similar results.

The magnetically dispersed axis provides the spectrum of the beams (see [16]), whereas the orthogonal axis provides a direct measure of the beam divergence. A spectrally resolved measurement of the beam divergence can thus be obtained in a single shot and it is depicted in figure 3 for 4.1 mm of Ta (2.8 mm of Ta provided similar results). As we can see, a divergence of the order of 3–4 mrad is obtained, with higher energy positrons being expelled in a narrower cone than the lower energy ones. This must be expected, since a multi-step cascade is unlikely for this range of target thicknesses and, therefore, the average positron beam divergence scales as $\theta_e^+ \approx 1/\gamma_e^+$ (see full blue circles in figure 3), being γ_e^+ the Lorentz factor of the escaping positrons. It is worth noticing here that this measured positron divergence is two orders of magnitude smaller than that obtained in [7] with a much more energetic laser (1 kJ compared to 0.8 J used in our experiment). It is remarkable also that such a relatively cheap device (a 1 J laser system like the one used in this experiment is now commercially available) can generate collimated positron beams with a density that is only two orders of magnitude smaller than the one obtained in the 2.4 mile long linear accelerator in SLAC (compare $n_e^+ \approx 2 \times 10^{14}\,\mathrm{cm}^{-3}$ reported in [16] with $n_e^+ \approx 5 \times 10^{16}\,\mathrm{cm}^{-3}$ reported in [2]).

For realistic laboratory-based astrophysical studies, it is though necessary to obtain higher positron densities whilst preserving their narrow divergence. In order to do so, two different approaches can be adopted: either the energy and number of the primary electrons can be increased, or a thicker target can be used (see section 2, in which it is predicted that the maximum positron yield is obtained for a target thickness of the order of twice the radiation length). An experiment was then carried out at the Astra-Gemini laser [18], which can provide laser pulses with much higher energy (up to 15 J, compared to 0.8 J) and thus electron beams with higher charge and energy. The main results of this campaign will be discussed in the next section of the article.

4. Positron beam divergence if $\delta > 1$

As mentioned at the end of the previous section, a straightforward way to increase the density and maximum

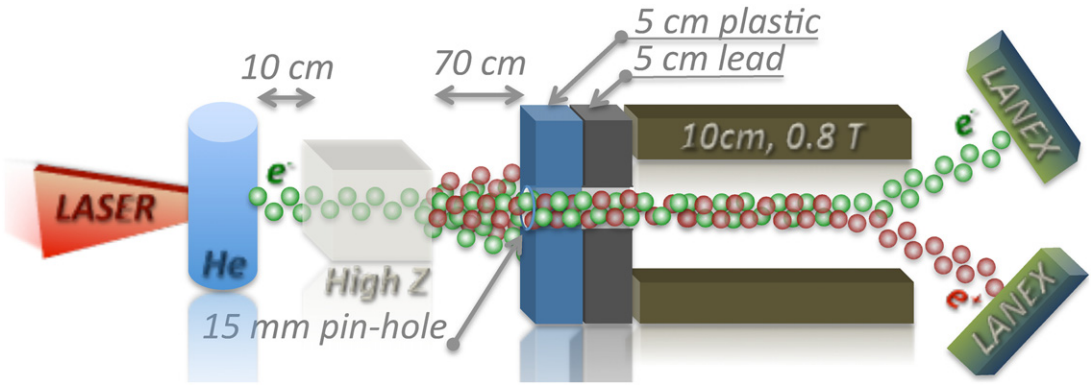

Figure 4. Sketch of the experimental setup adopted at the Gemini laser. The magnet is drawn tilted by 90°, for the illustration purposes. The setup closely resembles the one adopted in HERCULES (see figure 2) with the only differences that a higher energy laser pulse ($E_L \simeq 15$ J) and a longer and less dense gas-jet (20 mm, $n_e \simeq 2 \times 10^{18}$ cm^{-3}) were used.

energy of the positron beam is to increase the overall charge and energy of the primary electron beam. This can be easily achieved if more energetic laser pulses are used. Another experimental campaign was thus carried out at the Astra-Gemini laser [18], hosted by the Central Laser Facility at the Rutherford Appleton Laboratory, UK. This system can ensure laser pulses with a duration of 40 fs and an energy of the order of 15 J (i.e. more than fifteen times higher than that used in HERCULES, see previous section). Indeed, experimental results obtained using the Astra-Gemini laser have recently demonstrated the possibility of generating ultra-relativistic electron beams with maximum energy of the order of the GeV and overall charge of the order of hundreds of pC (associated number of electrons of the order of 10^9–10^{10}) [19]. The setup adopted in this experimental campaign was thus essentially identical to the one shown in figure 2, with the only difference that a higher energy laser pulse and a lower density gas-jet were used (see figure 4). In order to ensure a stable and high-charge electron beam, the gas-jet pressure was chosen so that it was higher than threshold for ionization injection [17]. A 20 mm long gas-jet (97% He, 3% N_2) with a backing pressure of 45 bar (corresponding, once fully ionized, to an electron density of the order of 5×10^{18} cm^{-3}) was thus used. This allowed generating a higher energy electron beam (see figure 5 for a typical electron spectrum as arising from the laser–gas interaction). The maximum energy of the electron beam was consistently of the order of 600 MeV and the charge carried by electrons with energy exceeding 160 MeV was of the order of 300 pC, with a shot-to-shot fluctuation within 10%. The divergence angle of the laser-accelerated electrons was in this case slightly higher than the one discussed in the previous section, having a full-width half-maximum of 2 mrad. In this experiment we again tried different materials (Ta, Pb, Mo, Sn) of different thicknesses (from a few mm up to a few cm). However, for the sake of this article, we will discuss here only the targets that ensured the highest positron yield, i.e. Pb. For this material, we studied the electron beam interaction with targets with a thickness of 0.5, 1, 2 and 4 cm which roughly correspond to 1, 2, 4 and 8 radiations lengths. Also in this case, positron beams with a monotonically decreasing spectrum were obtained, similarly to those reported in [16], yet with a higher number and maximum energy. A detailed

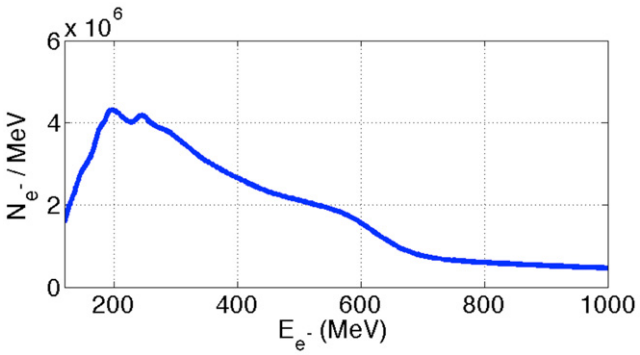

Figure 5. Typical electron spectrum as arising from the laser–gas interaction in the Astra-Gemini experiment. The maximum energy of the electron beam was consistently of the order of 600 MeV and the charge carried by electrons with energy exceeding 160 MeV was of the order of 300 pC with a shot-to-shot fluctuation of the order of 10%.

discussion of the positron spectra obtained in this experiment will be reported elsewhere [20], and we will focus here our attention only on the beam divergence, main focus of this article.

The divergence of the positron beam for these target thicknesses is plotted, as a function of the positron energy, in figure 6(*a*). It must be noted that the acceptance angle of the spectrometer was of the order of 8 mrad. It was thus impossible to directly measure any divergence larger than this value; therefore, the experimental points are limited to this range (empty squares, solid circles, and empty circles in figure 6(*a*)) whereas the solid lines arise from matching FLUKA simulations [21]. These simulations were performed assuming an initial electron beam with a spectral shape as the one depicted in figure 5 impacting onto a Pb target of the required thickness. 10^6 electrons were simulated, and every single simulation point is the result of an average over five identical runs, in order to minimize any stochastic error arising from the random seed generator of the code. The output of the simulation was then cross-checked by comparing the simulated and experimentally measured positron and electron spectrum at the exit of the solid target [20]. The good agreement between these two quantities indicated a good reliability on the simulated positron divergence. As we can see, the divergence effectively increase as the target thickness

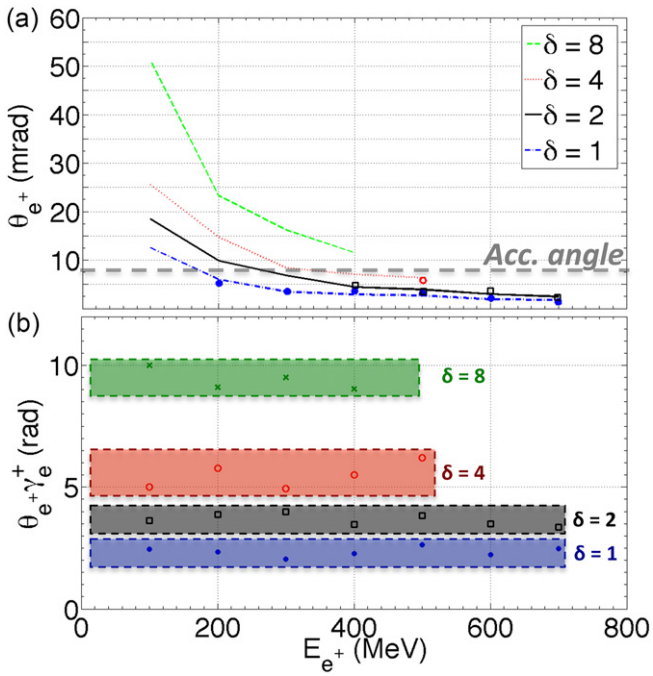

Figure 6. (*a*) Spectrally resolved divergence of the positron beam for different target thicknesses. Lines depict the divergence as obtained by matching FLUKA simulations, whereas the solid circles, empty squares, and empty circles depict the experimentally measured values for target thicknesses of $\delta = 1$, $\delta = 2$, and $\delta = 4$, respectively. (*b*) Product $\theta_{e^+}\gamma_{e^+}$ for different target thicknesses. For each target thickness, the product remains approximately constant, clear indication of the inverse proportionality between the divergence angle and the Lorentz factor of the particles.

is increased, but it is still of the order of 10–20 mrad for $\delta \leqslant 4$. In order to check the inverse proportionality with the particle Lorentz factor, the product $\theta_{e^+}^{+}\gamma_{e^+}^{+}$ is plotted, as a function of the particle energy, in figure 6(*b*). As we can see this inverse proportionality is well respected for all target thicknesses, and the divergence is also roughly proportional to $\sqrt{\delta}$, in good agreement with equation (6). It is worth noticing that targets thicker than twice the radiation length do neither provide an increase in positron yield (see discussion in section 2) nor in maximum energy. Moreover, they induce, due to a higher order cascade and increased probability of scattering, a significantly wider divergence. It is thus clear that the optimum properties of the positron beam (density, maximum energy, and divergence) can be achieved only for $\delta \approx 2$. For this case, we obtain: $\theta_{e^+}\gamma_{e^+} \approx 3$–4 rad. This value allows us to estimate the normalized emittance of the beam. In a first approximation, this can be expressed, at the exit of the solid target, as $\zeta_{e^+} \approx \theta_{e^+}\gamma_{e^+}D_{e^+}$, being D_{e^+} the beam source size. This latter value is, according to FLUKA simulations, of the order of 100 μm for $\delta = 2$. The normalized emittance can then be estimated as: $\zeta_{e^+} \approx 100\pi$ mm mrad. This value is comparable to that obtained in LEP ($\zeta_{LEP} = 60\pi$ mm mrad) [1] and could be further improved if primary electrons with a narrower divergence could be used.

5. Conclusions

We have reported on an experimental study of the divergence of laser-driven ultra-relativistic positron beams. For optimum experimental parameters, a beam divergence of a few mrad is obtained, resulting in a positron beam normalized emittance that is comparable to that achieved in large conventional accelerators such as LEP. Such a relatively low divergence suggests the possibility of implementing plasma afterburners for further acceleration of the positrons, towards the construction of a small-scale, plasma-based high-energy positron beam-line. This would be beneficial not only for fundamental nuclear and particle physics studies but also for laboratory-scale studies of astrophysical plasmas.

Acknowledgments

The authors are grateful for all the support received by the staff of the Central Laser Facility. The authors also acknowledge the funding schemes NSF CAREER (Grant No 1054164) and NSF/DNDO (Grant No F021166). GS wishes to acknowledge the support from the Leverhulme Trust (Grant No ECF-2011-383). ADP is grateful to AI Milstein and to AB Voitkiv for stimulating discussions.

References

[1] Bossart R *et al* 1990 *Report No* CERN-PS-90-56-LP
[2] Ng J S T *et al* 2001 *Phys. Rev. Lett.* **87** 244801
Blue B E *et al* 2003 *Phys. Rev. Lett.* **90** 214801
[3] Leemans W P *et al* 2006 *Nature Phys.* **2** 696
[4] Wang X *et al* 2013 *Nature Commun.* **4** 1
[5] Lu W *et al* 2007 *Phys. Rev. ST Accel. Beams* **10** 061301
[6] Blumenfeld I *et al* 2007 *Nature* **445** 741
[7] Chen H *et al* 2009 *Phys. Rev. Lett.* **102** 105001
Chen H *et al* 2010 *Phys. Rev. Lett.* **105** 015003
[8] Gahn C *et al* 2000 *Appl. Phys. Lett.* **77** 2662
Gahn C *et al* 2000 *Phys. Plasmas* **9** 987
[9] Esarey E, Schroeder C B and Leemans W P 2009 *Rev. Mod. Phys.* **81** 1229
[10] Blandford R D and Znajek R L 1977 *Mon. Not. R. Astron. Soc.* **179** 433
Goldreich P and Julian W H 1969 *Astrophys. J.* **157** 869
Wardle J F C *et al* 1998 *Nature* **395** 457
[11] Rossi B 1952 *High-Energy Particles* (New York: Prentice-Hall)
[12] Koch H W and Motz J 1959 *Rev. Mod. Phys.* **31** 920
[13] Beresteskii V B, Lifshitz E M and Pitaevskii L P 2008 *Quantum Electrodynamics* (Oxford: Butterworth-Heinemann)
[14] Scott W T 1963 *Rev. Mod. Phys.* **39** 231
[15] Yanovsky V *et al* 2008 *Opt. Express* **16** 2109
[16] Sarri G *et al* 2013 *Phys. Rev. Lett.* **110** 255002
[17] Clayton C E *et al* 2010 *Phys. Rev. Lett.* **105** 105003
[18] Hooker C J *et al* 2006 *J. Physique IV* **133** 673
[19] Kneip S *et al* 2009 *Phys. Rev. Lett.* **103** 035002
[20] Sarri G *et al* 2013 submitted
[21] Battistoni G *et al* 2007 *AIP Conf. Proc.* **896** 31